Inorg. Chem. **2005**, *44*, 8587–8593

Heme Axial Methionine Fluxion in *Pseudomonas aeruginosa* Asn64Gln Cytochrome c_{551}

Xin Wen and Kara L. Bren*

Department of Chemistry, University of Rochester, Rochester, New York 14627-0216

Received June 15, 2005

Heme axial methionine ligands in ferricytochromes c_{552} from *Hydrogenobacter thermophilus* (HT) and *Nitrosomonas europaea*, both members of the cyt c_8 family, display fluxional behavior. The ligand motion, proposed to be inversion at sulfur, results in an unusually small range of hyperfine shifts for heme substituents in these proteins. Herein, heme axial Met fluxion is induced in a structurally homologous cytochrome c_{551} from *Pseudomonas aeruginosa* (PA) by substituting heme pocket residue Asn64 with Gln. The mutant, PA-N64Q, displays a highly compressed range of heme substituent hyperfine shifts, temperature-dependent heme methyl resonance line broadening, low rhombic magnetic anisotropy, and a magnetic axes orientation consistent with Met orientational averaging. Analysis of NMR properties of PA-N64Q demonstrates that the heme pocket of the mutant resembles that of HT. This result confirms the importance of peripheral interactions and, in particular, residue 64 in determining axial Met orientation and heme electronic structure in proteins in the cyt c_8 family.

Cytochromes *c* (cyts *c*) are ubiquitous electron-transfer proteins that function in respiration and photosynthesis.[1,2] In the oxidized Fe(III) state, the NMR spectra of most cyts *c* feature a number of well-resolved, hyperfine-shifted resonances, the chemical shifts and assignments of which depend on heme electronic structure. In particular, the four heme methyls (at positions 1, 3, 5, and 8 shown using Fisher nomenclature in Figure 1; IUPAC numbering is 2, 7, 12, and 18) have been a focus of many NMR studies of low-spin paramagnetic cyts *c*.[3] The heme methyl hyperfine shifts arise primarily through the contact mechanism and thus reflect the pattern of unpaired electron spin density on the heme macrocycle. This pattern in turn is determined largely by the type and orientation of the heme axial ligands;[3,4] in fact, the heme methyl shift pattern can be used to predict axial ligand orientations[5] and to refine ligand geometries in structures.[6]

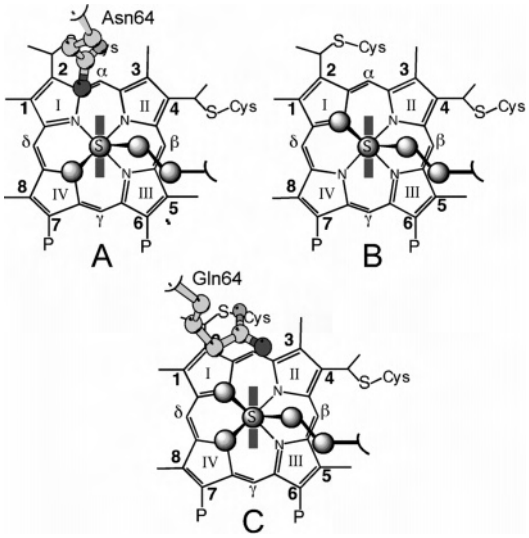

Figure 1. Side chain orientations of (A) heme axial Met and Asn64 in PA,[9] (B) heme axial Met in h-cyt *c*,[54] and (C) heme axial Met and Gln64 in HT.[18,19] The heme axial Met is sampling two conformations in (C). The Asn/Gln δ/ϵ N atom is in dark gray. The thick lines in gray indicate the orientation of the axial His, and P indicates propionate. The heme substituent and pyrrole numbering used in the text is indicated.

In cyts *c*, one of two axial Met conformations is commonly observed.[1−3] These conformations are illustrated in Figure

* To whom correspondence should be addressed. E-mail: bren@chem.rochester.edu.

(1) Scott, R. A.; Mauk, A. G. *Cytochrome c: A Multidisciplinary Approach*; University Science Books: Sausalito, CA, 1996.
(2) Moore, G. R.; Pettigrew, G. W. *Cytochromes c: Evolutionary, Structural, and Physicochemical Aspects*; Springer: Berlin, 1990.
(3) La Mar, G. N.; Satterlee, J. D.; de Ropp, J. S. Nuclear magnetic resonance of hemoproteins. In *The Porphyrin Handbook*; Kadish, K. M., Smith, K. M., Ruilard, R., Eds.; Academic Press: New York, 2000; Vol. 5, pp 185−298.
(4) Walker, F. A. *Coord. Chem. Rev.* **1999**, *186*, 471−534.
(5) Shokhirev, N. V.; Walker, F. A. *J. Biol. Inorg. Chem.* **1998**, *3*, 581−594.
(6) Bertini, I.; Luchinat, C.; Parigi, G.; Walker, F. A. *J. Biol. Inorg. Chem.* **1999**, *4*, 515−519.

10.1021/ic050976i CCC: $30.25
Published on Web 10/01/2005

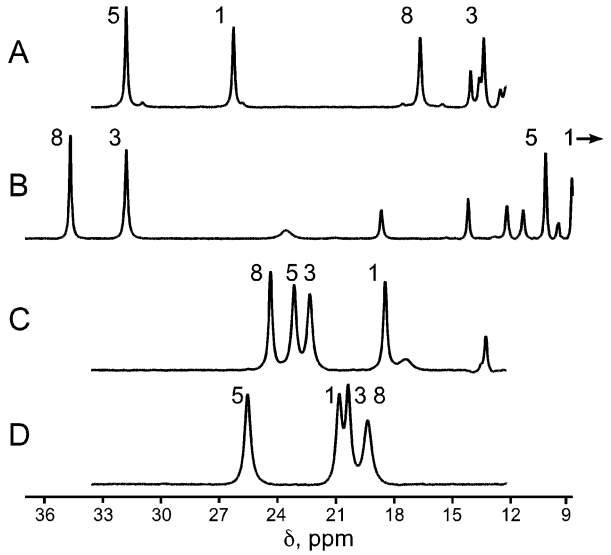

Figure 2. Downfield regions of ^{1}H NMR (500-MHz) spectra of oxidized (A) PA in 50 mM sodium phosphate, pH 6.0, 10% D_2O at 299 K,[15] (B) h-cyt *c* in 50 mM sodium phosphate, pH 7.0, 10% D_2O at 304 K,[15] (C) HT in 120 mM sodium acetate-d_3, pH 5.0, 10% D_2O at 299 K,[15] and (D) PA-N64Q in 50 mM sodium phosphate, pH 6.0, 10% D_2O at 299 K. Heme methyl resonance assignments are indicated.[13,46,55]

1A, B (the axial His in cyts *c* is typically aligned along the heme α−*γ*-meso axis).[7] Conformation A (Figure 1A) has a Met orientation[8] of ∼−15°, and conformation B (Figure 1B) has an orientation of ∼−71°.[9,10] These Met orientations result in different distributions of spin into heme π symmetry orbitals, yielding distinct heme substituent shift patterns and a typically large (∼20 ppm) spread of the heme methyl shifts. For conformation A, unpaired electron spin resides primarily in the heme $\Phi_y(3e\pi)$ orbital (the *y* axis is aligned with pyrroles I and III), directing spin to pyrroles I and III, resulting in larger chemical shifts for substituents on those pyrroles, and thus a heme methyl shift pattern in which methyls 5-CH_3 and 1-CH_3 have the largest chemical shifts (5-CH_3 > 1-CH_3 > 8-CH_3 > 3-CH_3; Figure 2A). Conformation B (Figure 1B), in contrast, has a shift pattern of 8-CH_3 > 3-CH_3 > 5-CH_3 > 1-CH_3 (Figure 2B), as a result of unpaired electron spin density residing primarily in the $\Phi_x(3e\pi)$ orbital.[11]

Given our understanding of the relationship between hyperfine shifts in low-spin ferriheme proteins and axial ligand orientations, reports of two cyts c_{552} with "anomalous" heme methyl shift patterns were surprising. These cyts c_{552} from *Hydrogenobacter thermophilus* (HT; Figure 2C) and *Nitrosomonas europaea* (NE) are unusual for showing neither of the canonical pairwise orderings of shifts.[12,13] Particularly striking is the compression of their heme methyl shift ranges (4.2 ppm for NE; 6.1 ppm for HT at 298 K).[12−15] These heme methyl shift patterns are not consistent with any orientation of the heme axial ligands.[5] Rather, it has been demonstrated that the heme methyl shift range compression in NE and HT arises from dynamics of the heme axial Met[14,15] (note that the axial His orientation is fixed by the Cys−X−X−Cys−His heme-binding motif that characterizes cyts *c*).[16] The axial Met in NE and HT is proposed to sample conformations A and B rapidly on the NMR time scale, leading to an averaged heme methyl shift pattern (Figure 1C; Figure 2C).[14,15]

The structural basis for the axial Met fluxion in HT has been explored by comparison of HT and *Pseudomonas aeruginosa* cytochrome c_{551} (PA), a structural homologue of HT with 70% sequence similarity but with an axial Met ligand fixed at an angle of −15°.[9,17] A seemingly subtle but critical difference in heme pocket structure between PA and HT is the presence of an Asn at position 64 in the former, and a Gln at position 64 in the latter. In PA, the Asn64 δ-NH_2 is oriented to interact with the axial Met61,[9] whereas in HT, the Gln64 side chain is oriented toward the protein surface and does not interact with heme pocket residues (Figure 1; numbering is based on the sequence of PA).[15,17−19] The hypothesis that residue 64 plays a crucial role in determining axial Met orientation and thus heme electronic structure in the cyts c_8 was tested by mutating Gln64 to Asn in HT.[17] The Q64N mutation successfully restricted the fluxional Met ligand in HT to a PA-like conformation, dramatically altering the downfield region of the ^{1}H NMR spectrum to yield a pattern strikingly similar to that of PA.[17] Nevertheless, the basis for the existence of axial Met fluxion in HT has not been revealed. One proposal is that the heme pocket in thermophilic HT exhibits strain as a result of rigidity of the Met-donating loop, thus raising the ground state so that the barrier for fluxion can be traversed at room temperature.[15] The existence of fluxion in NE, however, indicates that a protein need not be highly thermostable to exhibit this property.[14] Another hypothesis is that the intrinsic barrier to sulfur inversion at Met is low enough that fluxion will occur given enough space within the heme pocket.

In this work, the role of residue 64 in the cyt c_8 family and the basis for Met fluxion in some cyts *c* are explored further by introducing the N64Q mutation in PA. The heme

(7) Other axial Met orientations have been observed in cyts *c*. For example, see Costa, H. S.; Santos, H.; Turner, D. L. *Eur. J. Biochem.* **1994**, *223*, 783−789.
(8) For Met, the orientation angle is determined by projecting the bisector of the Met γC−δS−ϵC angle onto the heme plane and taking a vector perpendicular to this projection. The orientation angle of Met is the angle between this vector and the heme *x* axis. For His, the orientation angle is the angle between the ligand imidazole plane and the *xz* plane of the molecular coordinate system.
(9) Matsuura, Y.; Takano, T.; Dickerson, R. E. *J. Mol. Biol.* **1982**, *156*, 389−409.
(10) Bushnell, G. W.; Louie, G. V.; Brayer, G. D. *J. Mol. Biol.* **1990**, *214*, 585−595.
(11) Senn, H.; Wüthrich, K. *Q. Rev. Biophys.* **1985**, *18*, 111−134.
(12) Timkovich, R.; Cai, M. L.; Zhang, B. L.; Arciero, D. M.; Hooper, A. B. *Eur. J. Biochem.* **1994**, *226*, 159−168.
(13) Karan, E. F.; Russell, B. S.; Bren, K. L. *J. Biol. Inorg. Chem.* **2002**, *7*, 260−272.
(14) Bren, K. L.; Kellogg, J. A.; Kaur, R.; Wen, X. *Inorg. Chem.* **2004**, *43*, 7934−7944.
(15) Zhong, L.; Wen, X.; Rabinowitz, T. M.; Russell, B. S.; Karan, E. F.; Bren, K. L. *Proc. Natl. Acad. Sci. U.S.A.* **2004**, *101*, 8637−8642.
(16) Low, D. W.; Gray, H. B.; Duus, J. Ø. *J. Am. Chem. Soc.* **1997**, *119*, 1−5.
(17) Wen, X.; Bren, K. L. *Biochemistry* **2005**, *44*, 5225−5233.
(18) Hasegawa, J.; Yoshida, T.; Yamazaki, T.; Sambongi, Y.; Yu, Y.; Igarashi, Y.; Kodama, T.; Yamazaki, K.; Kyogoku, Y.; Kobayashi, Y. *Biochemistry* **1998**, *37*, 9641−9649.
(19) Travaglini-Allocatelli, C.; Gianni, S.; Dubey, V. K.; Borgia, A.; Di Matteo, A.; Bonivento, D.; Cutruzzolà, F.; Bren, K. L.; Brunori, M. *J. Biol. Chem.* **2005**, *280*, 25729−25734.

methyl shift pattern of PA-N64Q is dramatically changed to a compressed pattern such as observed in HT and NE. The magnetic axes orientation and magnetic anisotropy of PA-N64Q also resemble those determined for HT. These results underline the importance of residue 64 for determining axial Met orientation and heme electronic structure in cyts c_8 and demonstrate the ability to introduce axial Met fluxion into a cyt *c*.

Materials and Methods

Mutagenesis, Protein Expression, and Purification. Molecular biology procedures were generally as described by Sambrook et al.[20] The N64Q mutant of PA was prepared using the polymerase chain reaction overlap extension method.[21] A pET3c (Amp^r) vector (Novagen) containing the gene encoding the mature PA sequence preceded by its periplasmic translocation sequence[22] was used as the template for PCR amplification, and the mutagenic primers, 5′-GCCGCCGCAGGCGGTCAGC-3′ and 5′-CGCTGACCGCCTGCGGCGG-3′ (prepared by the Core Nucleic Acid Laboratory at the University of Rochester), were used (mutation site is underlined). The fresh PCR product was cloned into the pCR2.1 vector (TA cloning kit, Invitrogen). *Bam*HI and *Nde*I enzymes (Gibco BRL) were used to cleave the gene insert from pCR2.1 for ligation into pET17b (Amp^r) (Novagen). The Nova Blue strain of *Escherichia coli* (Novagen) was transformed with ligation reaction products under ampicillin selection, and the sequence was confirmed by DNA sequencing. The expression plasmid and the pEC86 (Cm^r) vector (harboring the *ccm* genes)[23] were used to transform BL21(DE3)-Star competent cells (Novagen) to chloramphenicol and ampicillin resistance. Expression and purification procedures for PA-N64Q were as described for wild-type PA.[22]

UV−Vis and CD Spectroscopy. Absorption measurements were made on a Shimadzu UV-2401PC photometer unit at ambient temperature. Spectra were obtained of oxidized (as purified) and reduced (excess $Na_2S_2O_4$ added) samples. Protein concentrations were determined using an extinction coefficient of 106 500 L mol^{-1} cm^{-1} at 410 nm, for oxidized PA and PA-Q64N.[24] Circular dichroism (CD) spectra were collected on a JASCO J-710 spectropolarimeter. Oxidized protein samples (1−2 mM) were in 50 mM sodium phosphate, pH 7.0, in a 0.100-cm path length quartz cell. Four scans at 200 nm/min with a 2-s response time and 2-mdeg or 5-mdeg sensitivity were collected for each sample from 615 to 725 nm at a 0.5-nm step resolution.

NMR Spectroscopy. ^{1}H NMR spectra were collected on a Varian INOVA 500-MHz spectrometer. Protein samples (2−3 mM) were in 50 mM sodium phosphate, pH 6.0, with 10% D_2O. Oxidized samples contained 5-fold molar excess $K_3[Fe(CN)_6]$. Reduced samples contained 20- to 30-fold molar excess of $Na_2S_2O_4$, which was added after flushing the sample with nitrogen gas. For oxidized PA-N64Q, two-dimensional (2-D) total correlation spectroscopy (TOCSY) and 2-D nuclear Overhauser effect spectroscopy (NOESY) spectra were collected at 299 K with 8192 points in the F2 dimension, 512 increments in the F1 dimension, and a 30 000-Hz spectral width. For reduced PA-N64Q, 2-D TOCSY and NOESY spectra were collected at 299 K with 4096 points in the F2 dimension, 512 increments in the F1 dimension, and a 12 000-Hz spectral width. The TOCSY spin-lock time was 50 ms, and the NOESY mixing time was 100 ms. Variable-temperature 1-D NMR spectra were collected on oxidized protein samples in 50 mM sodium phosphate, pH 6.0 (298−324 K) or in phosphate buffer containing 20% (v/v) CD_3OD (271−295 K). T_1 values were determined by inversion−recovery experiments using the standard $180°-\tau-90°$ pulse sequence with variable interval τ at 283 and 324 K. NMR spectra were processed and analyzed using FELIX 97 (Accelrys).

Heme Proton Resonance Assignments. Heme proton resonance assignments for both oxidized and reduced PA-N64Q were determined by identifying connectivities between heme substituents in NOESY spectra and confirmed by identifying NOEs between heme substituents and nearby amino acid side chains following standard procedures.[25] Assignments of proton resonances for amino acids were made following standard procedures[26] and were assisted by comparison to the published assignments for HT[13,18] and PA.[12,22,27]

NMR Line-Shape Analysis. For line-shape analysis, the variable-temperature ^{1}H NMR spectra of oxidized PA-N64Q were processed using NUTS 2001 (Acorn NMR, Inc.) The 1-CH_3 and 5-CH_3 resonances (the 3-CH_3 and 8-CH_3 resonances excluded because of overlap) were simulated using the program WINDNMR (version 7.1.5).[28] The assumptions made and procedures used are as described in detail elsewhere.[15]

Magnetic Axes Determination. Experimental pseudocontact shifts (δ_{pc}^{obs}) for PA-N64Q were determined by taking the difference between the shift of a proton in the oxidized (δ_{ox}) and reduced (δ_{red}) states:[3,29]

$$\delta_{pc}^{obs} = \delta_{para} - \delta_{dia} = \delta_{ox} - \delta_{red} \quad (1)$$

where δ_{para} and δ_{dia} are the chemical shifts of a given proton in the paramagnetic and an isostructural diamagnetic molecule. The magnetic axes orientation and the axial ($\Delta\chi_{ax}$) and rhombic ($\Delta\chi_{rh}$) anisotropies of PA-N64Q were determined by finding the best fit of experimental pseudocontact shifts to eq 2, in which r', θ', Ω' are the position of a given nucleus in the molecular coordinate system, and $R(\alpha, \beta, \gamma)$ is the Eulerian rotation matrix transforming the molecule to the magnetic coordinates r, θ, Ω:[3,29]

$$\delta_{pc} = (1/12\pi r'^3)[\Delta\chi_{ax}(3\cos^2\theta' - 1) + (3/2)\Delta\chi_{rh}(\sin^2\theta'\cos^2\Omega')][R(\alpha, \beta, \gamma)] \quad (2)$$

The mutated residue 64 was excluded from this analysis. The procedure is described in detail elsewhere.[15] Experimental and calculated pseudocontact shifts used in the fit are reported in Table S1.

Results and Discussion

Protein Expression. The yield of PA-N64Q was ∼1.7 μmol protein per liter of culture, which is similar to that for wild-type PA (∼1.4 μmol/L).[22] The UV−vis absorption

(20) Sambrook, J.; Fritsch, E. F.; Maniatis, T. *Molecular Cloning: A Laboratory Manual*, 2nd ed.; Cold Spring Harbor Laboratory Press: New York, 1989.
(21) Ho, S. N.; Hunt, H. D.; Horton, R. M.; Pullen, J. K.; Pease, L. R. *Gene* **1989**, *77*, 51−59.
(22) Russell, B. S.; Zhong, L.; Bigotti, M. G.; Cutruzzolà, F.; Bren, K. L. *J. Biol. Inorg. Chem.* **2003**, *8*, 156−166.
(23) Arslan, E.; Schulz, H.; Zufferey, R.; Kunzler, P.; Thöny-Meyer, L. *Biochem. Biophys. Res. Commun.* **1998**, *251*, 744−747.
(24) Horio, T.; Higashi, T.; Sasagawa, M.; Kusai, K.; Nakai, M.; Okunuki, K. *Biochem. J.* **1960**, *77*, 194−201.
(25) La Mar, G. N.; de Ropp, J. S. NMR Methodology for Paramagnetic Proteins. In *Biological Magnetic Resonance: NMR of Paramagnetic Molecules*; Berliner, L. J., Reuben, J., Eds.; Plenum Press: New York, 1993; Vol. 12, pp 1−78.
(26) Wüthrich, K. *NMR of Proteins and Nucleic Acids*; Wiley: New York, 1986.
(27) Detlefsen, D. J.; Thanabal, V.; Pecoraro, V. L.; Wagner, G. *Biochemistry* **1990**, *29*, 9377−9386.
(28) Reich, H. J. http://www.chem.wisc.edu/areas/reich/plt/windnmr.htm.
(29) Emerson, S. D.; Lamar, G. N. *Biochemistry* **1990**, *29*, 1556−1566.

Table 1. Chemical Shifts of Selected ^{1}H Resonances of Heme, the Axial Met61, and Residue 64 in HT, PA, and PA-N64Q[a]

	HT		PA		PA-N64Q	
substituent	Fe(III)	Fe(II)	Fe(III)	Fe(II)	Fe(III)	Fe(II)
1-CH_3	18.16	3.68	26.53	3.69	19.75	3.70
3-CH_3	22.29	3.87	13.17	3.75	19.21	3.79
5-CH_3	22.89	3.32	31.51	3.31	25.50	3.32
8-CH_3	24.28	3.45	15.99	3.40	21.35	3.38
α-meso-H	1.54	9.80	8.89	9.85	1.32	9.72
β-meso-H	−0.42	9.37	−1.32	9.37	−0.88	9.33
γ-meso-H	9.07	9.42	6.66	9.36	8.94	9.36
δ-meso-H	−1.17	9.28	−3.08	9.23	−2.11	9.23
Met61 γH1	−12.8	−1.08	−8.0	−0.50	−7.7	−0.67
Met61 γH2	−20.2	−3.36	−40.8	−3.50	−28.9	−3.64
Met61 ϵ-CH_3	−17.2	−2.89	−17.1	−2.92	−19.8	−2.84
Asn/Gln64 δ/ϵ-NH1	8.81	6.37	13.46	3.18	9.43	6.34
Asn/Gln64 δ/ϵ-NH2	6.70	6.67	13.86	7.58	7.07	6.53

[a] Shifts are in ppm and measured at 299 K. The assignments for wild-type HT are from ref 13; the assignments for wild-type PA are from ref 22.

spectra of both oxidized and reduced PA-N64Q are very similar to those of wild-type PA, including the presence of a band at ~690 nm for the oxidized protein, which is accepted to be indicative of Met ligation to Fe(III) (not shown).[1,2,30] These data indicate that PA-N64Q has the expected properties of a *c*-type cytochrome, with heme−polypeptide thioether bonds intact, and axial His−Met ligation.

Heme Proton Resonance Assignments. Chemical shifts for selected heme protons, the axial Met61, and residue 64 for oxidized and reduced PA-N64Q are listed along with those for oxidized and reduced wild-type PA and HT in Table 1. The heme resonance assignments for reduced PA-N64Q are similar to those of reduced wild-type PA, indicating no significant structural perturbation of the heme was introduced by the mutation, as expected.

As readily seen by inspection of the downfield region of the ^{1}H NMR spectrum of oxidized PA-N64Q, the pairwise shift pattern and large spread of the heme methyl shifts seen for wild-type PA (Figure 2A) is dramatically changed by the N64Q mutation to a highly compressed pattern (Figure 2D) reminiscent of that observed in HT (Figure 2C) and NE (not shown).[14] This strongly suggests that oxidized PA-N64Q has a fluxional Met as is observed in HT.[15] Chemical shifts of the heme meso-H resonances for oxidized PA-N64Q also are changed significantly from their values in wild-type PA and are similar to the values in HT (Table 1). The meso-H shifts result from both contact and pseudocontact contributions, which are in turn related to the axial ligand orientations.[5] The heme ^{1}H chemical shifts thus suggest that oxidized PA-N64Q and HT have similar heme electronic structures and similar axial ligand orientations.

Axial His Orientation in Reduced PA-N64Q. The most likely cause of a change in all four heme methyl shifts by the N64Q mutation in PA (oxidized) is a perturbation to one or both axial ligands. The orientation of the axial His is defined by the Cys−X−X−Cys−His heme-binding motif[16] and is generally aligned long the heme α-γ-meso axis in cyts *c*.[1,2] Moreover, residue 64 is positioned over the opposite face of the heme relative to His16; thus, the N64Q mutation is not expected to affect the conformation of His16. The similarity between the chemical shifts of His16 in diamagnetic, reduced PA-N64Q, and wild-type PA (in parentheses)[22] supports this assumption: NH, 6.80 (6.81); αH, 3.68 (3.72); βH1, 0.84 (0.82); βH2, 0.18 (0.13); δNH1, 8.69 (8.72); ϵH, 0.60 (0.63); δH2, 0.81 ppm (0.72 ppm). Thus, analysis of similarities and differences between PA, PA-N64Q, and HT will focus on the axial Met61 and nearby heme pocket residue 64.

Axial Met Conformational Disorder in Reduced PA-N64Q. The axial Met in reduced PA-N64Q is readily identified by its characteristic ^{1}H chemical shift pattern affected by the heme ring current (Table 1). Axial Met orientation in reduced, diamagnetic cyts *c* can be evaluated by analyzing the NOEs between the axial Met protons and the heme substituents (because of efficient relaxation, these NOEs are difficult to detect and interpret in oxidized, paramagnetic cyts *c*).[11,31] It is straightforward to distinguish between the two most frequently observed conformations of the axial Met in reduced cyts *c* through NOEs.[11] When the Met ligand displays conformation A (Figure 1A), NOESY cross-peaks from the axial Met ϵ-CH_3 are observed to the heme γ-meso-H, δ-meso-H, and 8-CH_3 but not to the heme α-meso-H, 1-CH_3, or 2-thioether-H (i.e., this pattern is seen in PA).[3,11,14,27,31] In contrast, when the Met ligand displays conformation B (Figure 1B), NOESY cross-peaks from the axial Met ϵ-CH_3 are not expected to the γ-meso-H or 8-CH_3 but should be seen to the heme α-meso-H and δ-meso-H, 8-CH_3, and 2-thioether-H (as is seen in reduced horse cyt *c* (h-cyt *c*)).[32] In reduced HT, Met conformational disorder is suggested by the observation of NOEs characteristic of both conformations of the axial Met.[15] Similarly, in reduced PA-N64Q, NOEs characteristic of both Met conformations are detected, suggesting Met conformational disorder in this protein form as well (Figure 3, Figure S1). This contrasts with NOESY data for reduced PA, which indicate the presence only of conformation A.[15,27]

Axial Met Fluxion in Oxidized PA-N64Q. The heme methyl shift compression immediately apparent in the downfield region of the ^{1}H NMR spectrum of oxidized PA-N64Q relative to wild-type provides a strong indication that the axial Met samples more than one conformation rapidly on the NMR time scale, in analogy to the behavior of oxidized HT.[15] The observed heme methyl chemical shifts are approximated by an averaging of the shifts expected for conformations A and B, which we assume to be similar to those for PA and h-cyt *c* (Figure 2). This observation holds through a range of temperatures (data not shown).

Support for the proposal that the axial Met is undergoing chemical exchange is provided by analysis of the temperature dependence of the heme methyl resonance line widths. If

(30) Harbury, H. A.; Cronin, J. R.; Fabger, M. W.; Hettinger, T. P.; Murphy, A. J.; Myer, Y. P.; Vinogradov, S. N. *Proc. Natl. Acad. Sci. U.S.A.* **1965**, *54*, 1658−1664.

(31) Senn, H.; Keller, R. M.; Wüthrich, K. *Biochem. Biophys. Res. Commun.* **1980**, *92*, 1362−1369.

(32) Banci, L.; Bertini, I.; Huber, J. G.; Spyroulias, G. A.; Turano, P. *J. Biol. Inorg. Chem.* **1999**, *4*, 21−31.

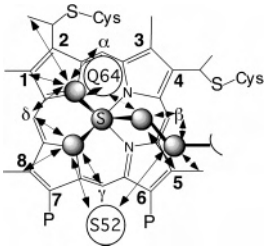

Figure 3. NOEs observed between the Met61 side chain and the heme and heme pocket amino acids Ser52 and Gln64 in reduced PA-N64Q. The NOEs are consistent with the existence of the two Met conformations shown.

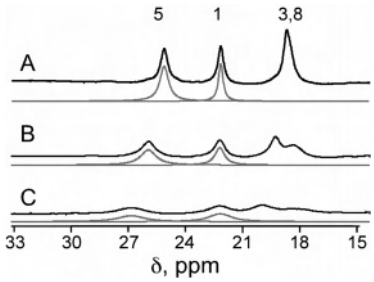

Figure 4. Downfield region of 500-MHz ^{1}H NMR spectra of oxidized PA-N64Q in 50 mM sodium phosphate, pH 6.0, 20% v/v CD_3OD, at variable temperatures. Underneath each spectrum is shown the simulated spectrum calculated in estimating the Met fluxion rate. Experimental temperatures and calculated exchange rates are (A) 294 K, 6.6×10^5 s^{-1}, (B) 284 K, 3.5×10^5 s^{-1}, and (C) 274 K, 1.9×10^5 s^{-1}.

the axial Met is undergoing fast conformational exchange near and above room temperature, at lower temperatures line broadening would be expected as the exchange rate approaches the intermediate exchange regime.[33] Indeed, such line broadening is seen as temperature is lowered for PA-N64Q (Figure 4, Figure S2). This behavior is similar to that reported previously for HT and NE but contrasts with PA, which shows minimal change in line width as temperature is decreased.[14,15] Importantly, unlike the resonance line widths, the T_1 values for the heme methyl protons in oxidized PA-N64Q show little variation with temperature (Table S2, Figure S2), which indicates that the broadening of the PA-N64Q heme methyl resonances is dominated by a chemical exchange process.[34]

Further analysis of the temperature-dependent line broadening observed for oxidized PA-N64Q allows estimation of an exchange rate for the axial Met between conformations A and B. Figure 4 shows the experimental and simulated ^{1}H NMR spectra of oxidized PA-N64Q through a range of temperatures. The calculated exchange rates reveal a microsecond time scale process, as expected (Figure 4). The activation enthalpy ($\Delta H^{\ddagger}$) is 39.5 ± 2.0 kJ mol^{-1} for the exchange process determined from an Eyring plot (Figure S3) is similar to that determined for HT ($\Delta H^{\ddagger} = 41.9 \pm 5.5$ kJ mol^{-1}).[15] The heme methyl proton chemical shifts calculated for conformation B are similar to those of *Desulfovibrio vulgaris* Hildenborough cytochrome c_{553}, which has *R* chirality at the axial Met and a 8-CH_3 > 3-CH_3 > 5-CH_3 > 1-CH_3 chemical shift pattern but a different Met conformation from h-cyt *c*.[11,35]

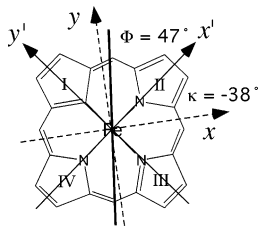

Figure 5. Orientation of magnetic axes in PA-N64Q. The solid arrows indicate the axes in the molecular reference frame (x', y', z'), and the dashed arrows are the magnetic axes (x, y, z), where x indicates the orientation of χ_{xx} for PA-N64Q. A solid line is positioned at the mean of the His and Met orientation angles in HT ($\Phi = 47°$). The parameter values determined for PA-N64Q by fitting δ_{pc}^{obs} data to eq 2 are $\alpha = 49°$, $\beta = 4°$, $\kappa = -38°$, $\Delta\chi_{ax} = 3.07 \times 10^{-32}$ m^3, $\Delta\chi_{rh} = -0.68 \times 10^{-32}$ m^3 determined for PA-N64Q.

A change in heme ligand orientation is expected to impact not only the shifts of the heme methyl resonances, which are dominated by the contact contribution to the hyperfine shift,[5,36] but also the magnetic axes orientation and possibly the magnetic anisotropy of the system, both of which can be determined by analysis of pseudocontact shifts.[3,29] The relationship between the magnetic axes and the axial ligand orientations in low-spin ferriheme proteins is described by the "counter-rotation rule."[3,37−39] In this formalism, if the mean axial ligand plane is oriented at an angle, Φ, from the molecular x axis (here, defined to be along the heme pyrrole II/IV N−Fe−N axis in the heme plane), the orientation of the minimum value principal χ axis (χ_{xx}) would be at angle $\kappa = -\Phi$ from that same axis (Figure 5). The value of κ, the in-plane rotation of the magnetic axes relative to the molecular axes, is determined by $\kappa = \alpha + \gamma$, where α and γ are Euler rotation angles that transform the molecular axes to the magnetic axes (eq 2), if there is no significant tilt of the magnetic z axis from the heme normal (i.e., the Euler angle β is small). For example, in PA, the value of Φ measured from its crystal structure is 15°; thus, the predicted κ value is −15°. The κ value determined by analysis of pseudocontact shifts for PA (−12°) is in good agreement with this predicted κ value.[15] In HT, the experimental value of κ (−47°) is consistent with the axial Met sampling conformations A and B as it is the average of the respective predicted (based on axial ligand orientations) κ values of −15° and −71°.[15]

Experimental and calculated pseudocontact shifts for PA-N64Q are reported in Table S1, and the plot of the resulting calculated and experimental pseudocontact shifts (δ_{pc}^{calc} vs δ_{pc}^{obs}) is shown in Figure S4. The resulting orientation of the χ tensor and anisotropies for PA-N64Q are reported in Figure 5 and Table S3. The κ value for PA-N64Q (−38°) changes relative to the value for wild-type and is consistent with axial Met conformational averaging, as it is similar to the average of the expected values for conformations A and

(33) Sandström, J. *Dynamic NMR Specctroscopy*; Academic Press: London, 1982.
(34) Burns, P. D.; Lamar, G. N. *J. Biol. Chem.* **1981**, *256*, 4934−4939.
(35) Blanchard, L.; Marion, D.; Pollock, B.; Voordouw, G.; Wall, J.; Bruschi, M.; Guerlesquin, F. *Eur. J. Biochem.* **1993**, *218*, 293−301.
(36) Lee, K.-B.; Lamar, G. N.; Mansfield, K. E.; Smith, K. M.; Pochapsky, T. C.; Sligar, S. G. *Biochim. Biophys. Acta* **1993**, *1202*, 189−199.
(37) Oosterhuis, W. T.; Lang, G. *Phys. Rev.* **1969**, *178*, 439−456.
(38) Shokhirev, N. V.; Walker, F. A. *J. Am. Chem. Soc.* **1998**, *120*, 981−990.
(39) Turner, D. L. *Eur. J. Biochem.* **1995**, *227*, 829−837.

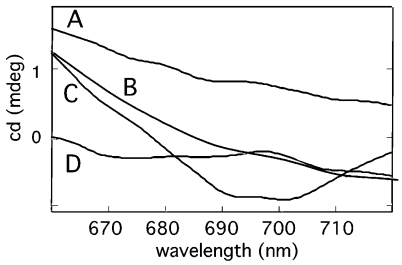

Figure 6. CD spectra of oxidized (A) HT (2.6 mM),[17] (B) PA-N64Q (2.0 mM), (C) h-cyt *c* (1.1 mM),[17] and (D) PA (1.5 mM)[17] at ambient temperature.

B (−47°). This result provides further support for the conclusion that the axial Met undergoes conformational exchange in PA-N64Q.

In addition to the magnetic axes orientation, the magnetic anisotropy of the system is altered by this mutation. The rhombic anisotropy calculated for PA-N64Q in the fit is -0.68×10^{-32} m^3, which is significantly smaller in absolute value from that for wild-type (-1.13×10^{-32} m^3). For bis-His or bis-imidazole iron porphyrins, a number of low-spin axial systems have been characterized.[40] The axial nature of these systems is a result of a perpendicular orientation of the two planar ligands. We propose an analogous effect is in place here. If the axial Met is rapidly sampling conformations A (Met angle ≈ −15°) and B (Met angle ≈ −71°), on the NMR time scale, the Met may be considered to have an average orientation ∼−43°. Because the His is oriented at +47°, the two axial ligands are effectively perpendicular to each other. Notably, the magnetic anisotropy of HT determined by NMR[15] and the EPR spectrum of NE[5,41] indicate low-spin axial electronic structures for these proteins.

The CD spectrum in the 690-nm region can be used to determine the chirality of the axial Met in class I ferricytochromes *c*.[11,31] In this region, a weak positive Cotton effect is observed for oxidized PA, which has *S* chirality at axial Met δS. In contrast, a negative Cotton effect is observed for oxidized h-cyt *c*, which has *R* chirality at Met δS (Figure 6).[31] In the case of HT, no distinct CD band is observed in this region, consistent with the existence of a mixture of Met chiralities.[15] Similarly, no observable band is seen in PA-N64Q, which is consistent with the presence of a mixture of *R* and *S* forms of the Met ligand.

Conformation of Residue 64 in Reduced PA-N64Q. Residue 64 in PA and HT takes different conformations relative to the heme and axial Met (Figure 1). In PA, the side chain of Asn64 is positioned over the center of the heme plane and is in contact with Met61 and Ile48 (which is positioned near heme δ-meso-H).[9] This conformation is seen in reduced PA by detection of NOEs between Asn64 δH1 and Met61 ϵ-CH$_3$ and γH2, and between Asn64 δH2 and the Ile48 side chain, as well as the heme 2-thioether-H.[15] In addition to these interresidue NOEs, the position of Asn64 is indicated by the upfield shift of Asn64 δH1 (the δ-NH$_2$ proton closer to the Met δS) from its expected value of ∼6−8 ppm[26] to 3.18 ppm in reduced PA, resulting from the heme ring current (note that no other aromatic groups are in the vicinity to cause this effect).[9,15,42] Indeed, the Asn64 NH$_2$ proton that interacts with the heme axial Met has an unusual shift of ∼3 ppm in all reduced cyts c_8 with an Asn64 characterized by NMR to date.[17,43−45]

In contrast to Asn64 in PA, the side chain of Gln64 in HT points to the periphery of the heme and NOEs from Gln64 to Ile48 are not observed.[15,18] NOEs are detected, however, between the Gln64 ϵ-NH$_2$ protons and the heme 3-CH$_3$, Pro62 γH and βH, and Met61 ϵ-CH$_3$, consistent with an orientation away from the heme iron. Consistent with the NOE pattern is that neither Gln64 ϵ-NH$_2$ proton experiences a significant heme ring current shift (δ = 6.37, 6.68 ppm).[13,15,18] The Gln64 ϵ-NH$_2$ resonances in reduced PA-N64Q have a pattern of NOEs and chemical shifts similar to those of HT. NOEs are not observed to Ile48, but NOEs are observed to the heme 3-CH$_3$, Pro62 γH and βH and Met61 ϵ-CH$_3$, i.e., the same as in HT (Figure S5). Gln64 in PA-N64Q also does not show a significant ring current shift for either ϵ-NH$_2$ proton (6.34, 6.57 ppm, Table 1). These data suggest that the side chain of Gln64 in PA-N64Q is positioned similarly to Gln64 in HT and the interaction between residue 64 and the axial Met is lost upon introducing the N64Q mutation into PA.

Conformation of Residue 64 in Oxidized PA-N64Q. As with reduced PA-N64Q, the position of the Gln64 side chain in the oxidized proteins can be assessed by analysis of NOEs and chemical shifts. The only non-intraresidue NOE observed from the Gln64 ϵ-NH$_2$ protons in oxidized PA-N64Q is to heme 3-CH$_3$. This is also the only NOE observed in oxidized HT and is consistent with orientation of Gln64 toward the heme periphery (Figure 1). The lack of other NOEs from Gln64 ϵ-NH$_2$ may be a result of mobility of Gln64, efficient relaxation of residues in the area by proximity to the heme iron, and/or a position at the surface of the protein away from other residues. It is also notable that the chemical shifts of the Gln64 ϵ-NH$_2$ protons in oxidized PA-N64Q are similar to those in oxidized HT and significantly changed from the values for Asn64 δ-NH$_2$ in wild-type. This observation is also consistent with the hypothesis that the heme active site structure and electronic structure of PA-N64Q mimics that of HT.

Conclusions

Bioinorganic chemists often assume that interactions between amino acid side chains and metals within metalloproteins can be described by a single conformation. Although this assumption is valid in most cases, we now have shown that fluxional behavior of a Met side chain ligated to a heme iron takes place in oxidized HT,[15] PA-N64Q (this work), and NE.[14] We also see conformational disorder of the axial Met in reduced HT[15] and PA-N64Q (this work). The basis

(40) Walker, F. A. *Chem. Rev.* **2004**, *104*, 589−615.
(41) Arciero, D. M.; Peng, Q. Y.; Peterson, J.; Hooper, A. B. *FEBS Lett.* **1994**, *342*, 217−220.
(42) Cross, K. J.; Wright, P. E. *J. Magn. Reson.* **1985**, *64*, 220−231.
(43) Timkovich, R.; Bergmann, D.; Arciero, D. M.; Hooper, A. B. *Biophys. J.* **1998**, *75*, 1964−1972.
(44) Cai, M.; Bradford, E. G.; Timkovich, R. *Biochemistry* **1992**, *31*, 8603−8612.
(45) Cai, M.; Timkovich, R. *Biophys. J.* **1994**, *67*, 1207−1215.

for Met fluxion in these proteins remains unknown, but we propose that simply having enough space available for the subtle side chain motion may be sufficient to allow this behavior. This hypothesis is consistent with induction of axial Met fluxion in the PA protein scaffold by replacing Asn64, which is buried within the heme pocket, with Gln64, which orients toward the protein surface, creating space near the axial Met. Indeed, a number of cyts *c* for which NMR spectra have been reported to be "normal" (i.e., the expected spread of heme methyl ^{1}H NMR shifts is observed for the oxidized form) and the structure is known exhibit packing of a heme pocket amino acid against the heme axial Met. For example, this is the case for h-cyt *c*,[10,46] *Monoraphidium braunii* cyt c_6,[47,48] *Rhodopseudomonas palustris* cyt c_2,[49,50] and *Thermus thermophilus* cyt c_{552}.[51,52] Gaining an understanding of factors that control axial Met orientation and fluxion, however, would require additional experiments on a range of cyts *c*, coupled with a more thorough analysis of available cyt *c* structures.

Inversion of thioether ligands in transition metal complexes is commonly observed at room temperature, and these motions are typically frozen out only at very low temperatures.[53] This raises the question as to why ligand fluxion, especially for Met ligands, is not more commonly observed within metalloproteins. The tightly packed nature of the interior of proteins may be the explanation. It also is possible that such behavior exists in metalloproteins other than HT and NE but has not been detected. For example, Met ligands to copper sites may undergo fluxion; however, this would be more difficult to detect spectroscopically than it is for ferric hemes. It is important to note that the X-ray crystal structure of oxidized HT reveals a single axial Met conformation (approximated by conformation B).[19] It is possible that the difference between behavior in the solution and crystalline forms of the protein results from crystal packing effects, as oxidized HT packs as a tetramer in the crystal, with Gln64 situated at an interface with another protomer. In addition, the low temperature for diffraction data collection on HT may favor the freezing out of a single conformation. Thus, determining ligand orientation on the basis of a crystal structure alone may result in errors in some cases.

In summary, PA-N64Q has been prepared and its heme pocket structure and electronic structure characterized to confirm the role of residue 64 in determining the Met ligand conformation and thus heme methyl shift patterns in cyts c_8. These results further demonstrate that site-directed mutagenesis is a powerful tool for altering heme electronic structure by perturbing peripheral interactions with the heme axial Met ligand conformation in cyts *c*. The availability of mutant cyts *c* with perturbed heme electron spin density distributions will allow systematic, controlled studies of the influence of heme pocket structure and electronic structure on heme electron-transfer reactivity.

Acknowledgment. This work was supported by National Institutes of Health Grant No. GM63170. K.L.B. is an Alfred P. Sloan Research Fellow.

Supporting Information Available: NMR data (Figure S1, S2, S5; Table S2, S3), Eyring plot (Figure S3), and experimental and calculated pseudocontact shifts (Table S1, Figure S4) for PA-N64Q. This material is available free of charge via the Internet at http://pubs.acs.org.

IC050976I

(46) Santos, H.; Turner, D. L. *FEBS Lett.* **1986**, *194*, 73−77.
(47) Campos, A. P.; Aguiar, A. P.; Hervas, M.; Regalla, M.; Navarro, J. A.; Ortega, J. M.; Xavier, A. V.; Delarosa, M. A.; Teixeira, M. *Eur. J. Biochem.* **1993**, *216*, 329−341.
(48) Banci, L.; Bertini, I.; De la Rosa, M. A.; Koulougliotis, D.; Navarro, J. A.; Walter, O. *Biochemistry* **1998**, *37*, 4831−4843.
(49) Geremia, S.; Garau, G.; Vaccari, L.; Sgarra, R.; Viezzoli, M. S.; Calligaris, M.; Randaccio, L. *Protein Sci.* **2002**, *11*, 6−17.
(50) Bertini, I.; Luchinat, C.; Macinai, R.; Martinuzzi, S.; Pierattelli, R.; Viezzoli, M. S. *Inorg. Chim. Acta* **1998**, *269*, 125−134.
(51) Than, M. E.; Hof, P.; Huber, R.; Bourenkov, G. P.; Bartunik, H. D.; Buse, G.; Soulimane, T. *J. Mol. Biol.* **1997**, *271*, 629−644.
(52) Fee, J. A.; Chen, Y.; Todaro, T. R.; Bren, K. L.; Patel, K. M.; Hill, M. G.; Gomez-Moran, E.; Loehr, T. M.; Ai, J. Y.; Thony-Meyer, L.; Williams, P. A.; Stura, E.; Sridhar, V.; McRee, D. E. *Protein Sci.* **2000**, *9*, 2074−2084.
(53) Toyota, S. *Rev. Hetero. Chem.* **1999**, *21*, 139−162.
(54) Berghuis, A. M.; Guillemette, J. G.; McLendon, G.; Sherman, F.; Smith, M.; Brayer, G. D. *J. Mol. Biol.* **1994**, *236*, 786−799.
(55) Timkovich, R.; Cai, M. L. *Biochemistry* **1993**, *32*, 11516−11523.